Draft version February 1, 2008
Preprint typeset using LaTeX style emulateapj v. 21/08/00

X-RAY SPECTRA OF INTERMEDIATE-LUMINOSITY, RADIO-LOUD QUASARS

Christa A. Hasenkopf, Rita M. Sambruna[1], and Michael Eracleous
Department of Astronomy & Astrophysics, The Pennsylvania State University, 525 Davey Laboratory, University Park, PA 16802
Draft version February 1, 2008

ABSTRACT

We present new hard X-ray spectra of three radio-loud AGNs of moderately high X-ray luminosity ($L_{\rm X} \approx 10^{45}$ erg s^{-1}; PKS 2349–01, 3C 323.1, and 4C 74.26) obtained with *ASCA* and *BeppoSAX*. The X-ray continua are described in all three cases with a power law model with photon indices $\Gamma \approx 1.85$, modified at low energies by absorption in excess of the Galactic, which appears to be due to neutral gas. At higher energies, an Fe Kα emission line is detected in PKS 2349–01 and 4C 74.26, and is tentatively detected in 3C 323.1. The equivalent widths of the lines are consistent, albeit within large uncertainties, with the values for radio-quiet AGN of comparable X-ray luminosity. The Fe Kα line is unresolved in 4C 74.26. In the case of PKS 2349–01, however, the inferred properties of the line depend on the model adopted for the continuum: if a simple power-law model is used, the line is resolved at more than 99% confidence with a full width at half maximum corresponding to approximately 50,000 km s^{-1} and a rest-frame equivalent width of 230 ± 120 eV, but if a Compton "reflection" model is used the line is found to be a factor of 2 weaker, for an assumed full width at half maximum of 50,000 km s^{-1}. In 4C 74.26, a strong Compton "reflection" component is detected. Its strength suggests that the scattering medium subtends a solid angle of 2π to the illuminating source. Overall, the spectral indices of these radio-loud quasars are remarkably similar to those of their radio-quiet counterparts. On the other hand, if the absorber is indeed neutral, as our results suggest, this would be consistent with the typical properties of radio-loud AGNs.

Subject headings: galaxies: active – X-rays: galaxies – quasars: individual (PKS 2349–01, 3C 323.1, 4C 74.26)

1. INTRODUCTION

A major outstanding question in our ongoing efforts to understand the central engines of active galactic nuclei (AGNs) is the origin of the dichotomy between radio-loud and radio-quiet objects. Although both radio-loud and radio-quiet AGNs are thought to be powered by accretion onto a supermassive black hole, it is not known why AGNs in the former class can produce collimated, relativistic radio jets, which power the giant radio lobes at large distances from their host galaxies, while AGNs in the latter class cannot (see Livio 1997, for a review). One possible explanation is that the central engines of the two classes of objects are the same, but systematic differences in the properties of the host galaxies are the cause of the observed dichotomy (e.g., Blandford & Levinson 1995; Fabian & Rees 1995). Another possibility is that there is a systematic difference between the central engines of radio-loud and radio-quiet AGNs, which is intimately related to their ability to form jets. Such a difference could be the size of the accretion disk (invoked in some wind models; e.g., Blandford & Payne 1982), the spin of the black hole (thought to be the ultimate power source of the jets; e.g., Blandford & Znajek 1977; Wilson & Colbert 1995; Meier 1999), or the structure of the inner accretion disk (an ion torus or advection-dominated accretion flow, a.k.a. ADAF, which allows some of the accreting matter to form an outflow; e.g., Rees et al. 1982; Narayan & Yi 1995; Blandford & Begelman 1999).

X-ray observations are a means by which one can investigate the last two of the above possibilities, since the X-rays are produced in the inner regions of the accretion flow. In particular, one can look for systematic differences in the X-ray spectral properties of radio-loud and radio-quiet AGNs that may indicate differences in the structure of the inner accretion disk or the spin of the central black hole. Thus we and other groups have been carrying out systematic studies of the X-ray properties of radio-loud AGNs using archival as well as proprietary *ASCA* and *RXTE* observations. These studies have confirmed previously suspected systematic differences between radio-loud and radio-quiet AGNs (Zdziarski et al. 1995; Woźniak et al. 1998; Sambruna, Eracleous, & Mushotzky 1999; Eracleous, Sambruna, & Mushotzky 2000). In particular, two spectral features that are the hallmarks of the X-ray spectra of Seyfert galaxies (e.g., Nandra & Pounds 1994; Nandra et al. 1997b): the fluorescent Fe Kα line at 6.4 keV and the Compton "reflection" hump at energies greater than 10 keV, are considerably weaker in the spectra of broad-line radio galaxies (hereafter BLRGs; Zdziarski et al. 1995; Woźniak et al. 1998; Sambruna et al. 1999; Eracleous et al. 2000). The above observational results suggest that the structure of the inner accretion disk of BLRGs is different from that of Seyfert galaxies, although the nature of this difference remains to be understood in detail. Another potentially important trend is the X-ray Baldwin effect (Nandra et al. 1997c), according to which the Fe Kα lines of luminous quasars are systematically weaker (i.e., of lower equivalent width; hereafter EW) than those of

[1] Current address: Department of Physics & Astronomy and School of Computational Science, George Mason University, Fairfax, VA 22030

the lower-luminosity Seyfert galaxies. Because the sample of objects studied by Nandra et al. (1997c) includes a mix of radio-loud and radio-quiet quasars (hereafter QSRs and QSOs, respectively), it is not yet clear whether and how such an effect applies to radio-loud and radio-quiet AGNs separately. Finally, the immediate environment of the X-ray source appears to be different in radio-loud and radio quiet AGNs as evidenced by the properties of absorbing material along the line of sight. More specifically, the signature of a "warm" (i.e., ionized) absorber, seems to be ubiquitous in Seyfert galaxies (e.g., Reynolds 1997; George et al. 1998) but rare in broad-line radio galaxies (Sambruna et al. 1999). Instead, radio-loud AGNs seem to display the signature of significant absorption by neutral matter in their X-ray spectra.

Here we present the results of new observations of three intermediate-luminosity QSRs (3C 323.1, PKS 2349–01, 4C 74.24; $L_{\rm X} \sim 10^{45}$ erg s^{-1}) with *ASCA* and *BeppoSAX*, which were carried out as part of our larger program. The targets were specifically selected to bridge the gap in luminosity between the nearby and well-studied BLRGs and the more luminous QSRs included in the sample of Nandra et al. (1997c). All three are associated with large, double-lobed radio sources (Antonucci 1985; Kellerman et al. 1994; Riley et al. 1988), which ensures that our line of sight is not close to the axis of their radio jet, thus the X-rays we observe are not contaminated by beamed emission from the jet itself. The goal of the observations was to investigate the properties of intermediate-luminosity QSRs and to check whether the systematic differences between Seyfert galaxies and BLRGs extend to higher luminosity objects. In this respect, 4C 74.26 is a particularly interesting object because its *ASCA* X-ray spectrum (Brinkmann et al. 1998; Sambruna et al. 1999) showed features that are hallmarks of Seyfert galaxies but not BLRGs: a "warm" absorber with a column density of 3.5×10^{21}cm^{-2} and a significant Compton "reflection" hump. It was also the only QSR in the collection of Sambruna et al. (1999) with a detectable Fe Kα line.

In §2 we describe the observations and basic data analysis while in §3 we present the results of fitting models to the spectra. In §4 we discuss our results and we present our final conclusions. Throughout this paper we adopt a Hubble constant of $H_0 = 50$ km s^{-1} Mpc^{-1} and a deceleration parameter of $q_0 = 0.5$.

2. OBSERVATIONS, DATA SCREENING, AND TIMING ANALYSIS

ASCA observations of PKS 2349–01 and 3C 323.1 were carried out in 1999 December and 2000 February, respectively. Table 1 reports the observation log. The SIS detectors were operated in `1-CCD FAINT` mode half of the time and in `1-CCD BRIGHT` mode for the remaining portion, while the GIS detectors were operated in `PH` mode. The data were screened within `FTOOLS/XSELECT v.4.2` (Blackburn, Greene, & Pence 1994; Ingham 1994) following the procedures described in Eracleous & Halpern (1998) and Eracleous et al. (1996). The final net exposure times are included in Table 1. After screening, we extracted spectra and light curves for each of the *ASCA* detectors. The `FAINT` mode data were converted into `BRIGHT2` mode and combined to the `BRIGHT` mode data, to take advantage of the full exposure time and maximize the signal-to-noise ratio (S/N).

4C 74.26 was observed in 1999 May (Table 1) by the *BeppoSAX* narrow field instruments: the Low- and Medium-Energy Concentrator Spectrometers, and the Phoswich Detector System (hereafter LECS, MECS, and PDS, respectively). The data from two of the three MECS units were merged to increase the S/N. The exposure times resulting from the application of standard screening criteria to account for passage through the South-Atlantic Anomaly, Earth occultation, etc. (Fiore et al. 1999), are listed in Table 1. The source was detected in the PDS band up to energies of order 100 keV, with a count rate of 0.52 ± 0.04 c s^{-1} (Table 1). No bright sources were found in the LECS and MECS fields of view, thus enhancing our confidence that the source detected by the PDS is indeed the target quasar.

Figure 1 shows the *ASCA* and *BeppoSAX* light curves of the three targets. For PKS 2349–01 and 3C 323.1, we show the 2–10 keV light curves from the two *ASCA* GIS detectors combined, binned at 30-minute intervals. For 4C 74.26, we show the 2–10 keV light curve from the MECS instrument, binned at 30-minute intervals, as well as the 15–125 keV light curve from the PDS instrument, binned at 2-hour intervals. No systematic variability is evident in any of the light curves save for a brief, 25% excursion in the case of PKS 2349–01. To search for short-time scale fluctuations we applied the excess variance test (Nandra et al. 1997a; Turner et al. 1999) to the light curves binned at both 256-second and 1800-second intervals. The excess variance measured from the 256-second light curves is $(5.4 \pm 0.1) \times 10^{-2}$ s^{-1}, $(5.5 \pm 0.3) \times 10^{-2}$ s^{-1}, and $(4.2 \pm 0.1) \times 10^{-2}$ s^{-1} for PKS 2349–01, 3C 323.1, and 4C 74.26, respectively. These values are higher than those of Seyfert galaxies of comparable luminosity (see, for example Leighly 1999; Turner et al. 1999) but they are similar to the values found for narrow-line Seyfert 1 galaxies of comparable luminosity. The corresponding values of the excess variance for the 1800-second light curves are $(5.8 \pm 0.1) \times 10^{-2}$ s^{-1}, $(3.7 \pm 0.1) \times 10^{-2}$ s^{-1}, and $(1.8 \pm 0.1) \times 10^{-2}$ s^{-1} for PKS 2349–01, 3C 323.1, and 4C 74.26, respectively. The observed fluctuations are unlikely to be related to emission from the jets of these objects because the radio morphology suggests that the the jets are oriented at large angles to the line of sight (Antonucci 1985; Kellerman et al. 1994; Riley et al. 1988). This conclusion is also supported by the high-energy light curve of 4C 74.26, which is rather steady over the course of the observation, in marked contrast to the light curves of blazars.

3. MODEL FITS TO THE SPECTRA

Models were fitted to the *ASCA* and *BeppoSAX* spectra using XSPEC v.11.0.1 (Arnaud 1996), in the energy ranges where the calibration is well established and the background is low (see Table 1). The spectra were rebinned such that each new bin contained at least 20 counts in order to validate the use of the χ^2 statistic. We used the most current versions of the response matrices and effective area curves (September 1, 1997 files for the *BeppoSAX* instruments; February 3, 1995 response matrices for the *ASCA* GIS, and all other *ASCA* calibration files

generated specifically for our observations).

To check the self-consistency of the spectra obtained by different *ASCA* detectors, we first fitted the individual SIS and GIS spectra. We then fitted the same model to the spectra from all detectors simultaneously. To take account of any uncalibrated differences between the effective areas of the different instruments, we allowed the normalization of the corresponding spectra to vary freely. An analogous procedure was adopted for the spectra from the *BeppoSAX* detectors, as we discuss further below. As with the *ASCA* spectra, the normalization constants of spectra from different instruments were also allowed to vary, but the PDS normalization was constrained to be between 0.77 and 0.83 of the MECS normalization. The best-fitting value for the PDS/MECS ratio was found to be $0.83^{+0}_{-0.06}$. The best-fitting LECS/MECS ratio, which was left free to vary, was 0.70±0.02.

The goals of the spectral analysis are to determine the model that best describes the continuum, including possible excess absorption at low energies and the Compton hump at $E \gtrsim 10$ keV, and check for the presence of the Fe Kα emission line. To determine the best-fitting continuum models, we adopted the following procedure. At first, the spectra were fitted by excluding the rest energy range 5–7 keV, where the Fe Kα line contributes most. Once the best-fitting continuum model was found, the 5–7 keV range was added back to the spectra and a Gaussian line was added to the model. This procedure ensures the continuum and the emission line remain unaffected by one another in the fitting process, an especially important concern if the line is broad (e.g., Nandra et al. 1997b).

While we investigated the presence of excess absorption at low energies in the three targets, a detailed analysis was possible only in the case of 4C 74.26, as the LECS sensitivity extends to lower energies than the SIS and the spectral calibration is more certain. For each *ASCA* detector we only use data in the energy range given in Table 1 in order to bypass calibration problems associated with the SIS efficiency loss at low energies (Yaqoob et al. 2000). Excluding the lowest-energy bins in the SIS spectra results in larger uncertainties in the determination of the absorbing column, however the column densities turn out to be high enough in both *ASCA* targets that they can be determined fairly well even by the GIS detectors. The presence of a Compton "reflection" hump can be determined with confidence only in the *BeppoSAX* data because of the higher-energy sensitivity of the PDS compared to the SIS and GIS detectors.

3.1. *The Continuum*

The best-fitting model for the *ASCA* spectra of PKS 2349–01 and 3C 323.1 is an absorbed power law with column density in excess of the Galactic value plus a Gaussian emission line. The best-fitting models, parameters, and corresponding error bars (at 90% confidence for two parameters of interest) are summarized in Table 2, while the spectra are shown in Figure 2 with models superposed. All the models include an absorption component, fixed to the Galactic column density, and a second absorption component (due to neutral gas) at the source's redshift with the column density left free to vary in the fit. The implicit assumption of this procedure is that any excess absorption is at the source's rest-frame. The simple power-law model also provides a good description of the LECS+MECS ($E < 10$ keV) spectrum of 4C 74.26 but it leaves large residuals at high energies, in the portion of the spectrum sampled by the PDS, as shown in Figure 2c.

It is noteworthy that the absorbing column detected in the spectrum of 4C 74.26 is rather high, namely 3×10^{21} cm^{-2}, a few times higher than what is measured for the other two objects. Analysis of the *ASCA* spectrum of this object by Brinkmann et al. (1998) suggested the presence of an intrinsic, ionized absorber ("warm" absorber). That result, however, was not confirmed in the independent analysis of the same data by Sambruna et al. (1999). To investigate this question further we fitted the LECS spectrum with two different models representing an ionized absorber: (a) a single power law with Galactic and intrinsic absorption, plus a redshifted absorption edge, and (b) an ionized absorber model according to Done et al. (1992, implemented by the XSPEC routine `absori`). In neither case did we find a significant improvement of the fit: the total value of χ^2 decreases because of the additional free parameters of these more sophisticated absorption models, but the improvement is significant only at the 50–65% level (according to the F-test). Our conclusion, therefore, is that although a warm absorber provides an acceptable fit, it is not required by the data.

The high-energy residuals in the simple power-law fit to the spectrum 4C 74.26 indicate the presence of an additional continuum component emerging at energies $\gtrsim 10$ keV. The following two possibilities were considered in detail:

1. The high-energy excess flux is due to Compton "reflection" of the primary continuum by neutral, dense matter in the immediate vicinity of the X-ray source (Lightman & White 1988; Guilbert & Rees 1988). Thus, we fitted the *BeppoSAX* spectrum with a Compton "reflection" model (`pexrav` within XSPEC Magdziarz & Zdziarski 1995). This model has several additional free parameters, which include the inclination angle, i, of the reprocessing slab relative to the line of sight, the solid angle, Ω, that the slab subtends to the primary X-ray source, and the upper cut-off energy of the primary power-law spectrum. In the particular case of 4C 74.26 we can use the radio properties to constrain the inclination angle of the radio jet (hence the inclination angle of the disk). The brightness contrast between the small-scale jet and counter-jet (observed by VLBI), if ascribed to relativistic beaming, yields an upper limit to the jet inclination angle of $i \leq 49°$ (Pearson et al. 1992). Requiring that the size of the large-scale radio source does not exceed the size of giant radio sources observed in radio galaxies can yield a lower limit on the inclination. Such giant radio source sizes typically range up to 2.0–2.5 Mpc (e.g., Palma et al. 2000; Lara et al. 2001). Assuming that the radio source in 4C 74.26 is not exceptionally large and adopting 2 Mpc as an upper limit to its true size, we obtain $i \geq 37°$. Thus we can express the inclination angle as $i = 43 \pm 6$ degrees. [2]

[2] The constraints on the inclination angle of the jet derive from ratios of fluxes or lengths; thus they do not depend on H_0.

In Table 2 we give the best fitting model parameters for the case where the inclination angle of the axis of the reprocessing slab was held fixed to the value inferred from the radio morphology. In Figure 4 we show how the inferred reprocessor solid angle depends on the value of the inclination by plotting the 68, 90, and 99% confidence contours in the $\cos i - \Omega/2\pi$ plane. For inclination angles between 37° and 49°, which represent the range inferred from the radio properties, the solid angle is consistent with 2π. The fit with the Compton "reflection" model is an improvement over the single power law at the 98.7% confidence level, according to the F-test.

2. The excess flux could indicate a contribution from the base of the jet. This was modeled by adding a second power law to the continuum, which did not yield a significantly different description, however, leading us to disfavor this option. More specifically, the spectral indices of the two power-law components converge to values that are indistinguishable from each other and the total χ^2 value is higher than the Compton "reflection" model, which has more free parameters. Moreover, emission from a jet is disfavored by the radio properties of this object (mainly the morphology), which suggest that the jet is oriented at a large angle to the line of sight ($i > 37°$).

Although the *ASCA* bandpass is not well-suited to the detection of the Compton "reflection" continuum, we nevertheless searched for it in the spectra of PKS 2349–01 and 3C 323.1. The main reason for embarking on this exercise is that the adopted continuum model could have an influence on the measured properties of the Fe Kα lines, which we study in the next section (see the discussion in the context of 4C 74.26 in §3.3). In the case of 3C 323.1 we find no evidence for a Compton "reflection" continuum. In fact, a Compton "reflection" model converges to a model with negligible "reflection," which is in effect the original simple power-law model. In the case of PKS 2349–01 the Compton "reflection" model results in a slightly lower χ^2 value than the simple power-law model, but this apparent improvement is not significant (the F-test gives a 66% probability of improvement by chance). But the two continuum models yield significantly different properties for the Fe Kα line, as we describe below. This effect has been known for some time, and has been discussed by a number of authors, including most recently Zdziarski & Grandi (2001).

3.2. *The Fe Kα Emission Line*

To search for the presence of an Fe Kα emission line, which is a ubiquitous feature of the X-ray spectra of Seyfert galaxies, we modeled its profile with a Gaussian. We fitted the continuum as described above and fixed the continuum parameters before adding the Gaussian line profile to the model. To evaluate whether the line is unambiguously detected and resolved we searched the 2-dimensional parameter space defined by the line photon flux and the energy dispersion of the Gaussian profile. The results of this search are shown in Figure 5 in the form of confidence contours in the line EW *vs* FWHM plane (the EW and FWHM are directly proportional to the line photon flux and Gaussian energy dispersion, respectively). These results are also summarized in Table 3.

In the case of 4C 74.26 the line is clearly detected with a rest EW of 170^{+180}_{-100} eV. The energy of the Fe Kα emission line encompasses the range 6.4 to 6.9 keV within 90% confidence. Thus, we confirm the detection of the line in 4C 74.26 with *ASCA*, as reported by Brinkmann et al. (1998) and Sambruna et al. (1999). In the case of 3C 323.1 the line is only marginally detected, i.e., its EW is non-zero at 90% confidence but consistent with zero at 99% confidence (for an assumed energy of 6.4 keV). The best-fitting FWHM is about 5×10^4 km s^{-1}, which is comparable with what is found in Seyfert galaxies by Nandra et al. (1997b).

In the case of PKS 2349–01, the measured properties of the Fe Kα line depend sensitively on the continuum model. If we adopt a simple power-law model, the line is unambiguously detected at the 99% confidence level with a rest EW of 230 ± 120 eV and a FWHM of $6^{+6}_{-3} \times 10^4$ km s^{-1}. If, however, we adopt a model consisting of a power-law plus Compton "reflection," fixing the solid angle of the reprocessor to $\Omega = 2\pi$, the line is about a factor of 2 weaker (see Table 3). If we fix the solid angle of the reprocessor to $\Omega = 4\pi$, its maximum physically reasonable value, the line is only marginally detected (at the 68% confidence level). The upper limit to its rest EW is 200 eV, assuming a FWHM of 5×10^4 km s^{-1}. This ambiguity cannot be resolved with the data at hand. In order to measure the properties of the Fe Kα lines with confidence, we need either a 2–10 keV spectrum of much higher S/N or a spectrum of comparable S/N extending to at least 30 keV, which can yield meaningful constraints on the properties of the Compton "reflection" component. Finally, we also note that the observed EWs of the Fe Kα lines and the strength of the Compton "reflection" components are consistent with each other, albeit within the large uncertainties, as one would expect in the context of reprocessing models such as those of George & Fabian (1991). Such models attribute the origin of both the Fe Kα line and the Compton "reflection" component to the same reprocessing medium and require that their strengths are related.

3.3. *Comparison With Previous Observations of 4C 74.26 by ASCA*

Our preferred model for 4C 74.26 consists of a power-law continuum modified by Compton "reflection" at high energies and by absorption at low energies. The line energy obtained from the model could not be tightly contrained, falling between 6.4 and 6.9 keV at a 90% confidence level. Within uncertainties, our results are largely consistent with the results of Brinkmann et al. (1998), who considered our preferred model among others. However, there is a systematic discrepancy between the properties of the Fe Kα line, which we attribute to the continuum fit used by Brinkmann et al. (1998). More specifically we find that the line is several times broader and about 70% stronger than what Brinkmann et al. (1998) found. Comparing the parameters describing the continuum, we see that the Compton "reflection" component in the *ASCA* spectrum of Brinkmann et al. is poorly constrained and has an extremely high value that implies the reprocessor

subtends an area larger than 3 times the area of the sky. Although this could be interpreted as an indication that the primary X-ray source does not emit isotropically, it is also possible that the strength of the Compton "reflection" component was overestimated.

Such poor constraints on the Compton "reflection" component are not surprising, since the *ASCA* sensitivity drops dramatically at $E > 8$ keV, making it practically impossible to measure this component. Thus, the continuum around the Fe Kα line is elevated, taking away the broad wings of the line and reducing its overall strength. In contrast, in our *BeppoSAX* spectrum we are able to determine the shape of the high-energy continuum unambiguously with the help of the PDS. We find a considerably weaker Compton "reflection" strength than Brinkmann et al. (1998) and a correspondingly broader and stronger Fe Kα line.

In view of the strength of the Compton "reflection" component measured from the *BeppoSAX* spectrum, we reanalyzed the the *ASCA* spectra to check for consistency. We extracted and fitted the spectra with the same methodology described in §2 and §3, keeping the Compton "reflection" component fixed to a strength corresponding to $\Omega = 2\pi$, as measured from the *BeppoSAX* spectrum. We measured the EW of the Fe Kα line for fixed rest energies of 6.4 and 6.7 keV. We found that the measurements from the *ASCA* spectra are consistent with those from the *BeppoSAX* spectrum. In particular, we measure a spectral index of $1.87^{+0.08}_{-0.07}$, while the Fe Kα rest EW is poorly constrained and lies in the range 130–700 eV, as listed in Table 3.

4. SUMMARY AND DISCUSSION

We have presented new *BeppoSAX* and *ASCA* observations of three luminous ($L_{2-10\ \mathrm{keV}} \sim 10^{45}$ erg s^{-1}) radio-loud AGN, as part of our ongoing systematic study of the X-ray properties of such objects. We find that in all three cases the main underlying continuum can be described as a power law with photon index $\Gamma \approx 1.85$, plus excess absorption. In two sources (PKS 2349–01 and 4C 74.26) the Fe Kα emission line is detected with rest-frame EW $\sim$ 200 eV but with large uncertainties, of a factor of 2; in 4C 74.26 the line is unresolved while in PKS 2349–01 the line properties depend on the model adopted for the continuum. In 4C 74.26, a strong ($\Omega \approx 2\pi$) Compton "reflection" component is also detected with the PDS instrument on *BeppoSAX*. In PKS 2349–01, on the other hand, the data allow the presence of a Compton "reflection" component but cannot provide meaningful constraints on its strength. This is unfortunate because the strength of this component affects the inferred properties of the Fe Kα line dramatically, as we explained in detail in §3.2.

The average photon index for the three sources studied here is $\langle\Gamma\rangle = 1.86$ with a small dispersion of $\sigma_\Gamma = 0.01$. The average slope of the X-ray continuum is consistent with the average photon index previously measured with *ASCA* for a small sample of 7 QSRs of comparable luminosity, which had $\langle\Gamma\rangle = 1.80$ and $\sigma_\Gamma = 0.15$ (Sambruna et al. 1999). This is also consistent with the average slope for a sample of radio-quiet quasars from *ASCA* measurements, $\langle\Gamma\rangle = 1.86$ and dispersion $\sigma_\Gamma = 0.20$ (see Table 5 of Sambruna et al. 1999). The similarity of slopes for the radio-loud and radio-quiet sources confirms that no contribution from the beamed emission of an unresolved jet is present in the radio-loud QSRs of our study (as expected based on their radio morphology, see above). It also suggests a similar continuum emission process in the two classes of AGN. This result will need to be confirmed using larger samples of both radio-loud and radio-quiet sources. Moreover, a wider spectral coverage will also be needed in order to constrain the strength of the Compton "reflection" hump and disentangle its effects from the slope of the intrinsic continuum.

Another result of this paper is the excess absorption found in all three objects. In 4C 74.26, where the observed spectra extend to low energies, we have searched for the signature of a warm absorber, but have not found conclusive evidence for it, nor were we able to rule it out. There are two possible origins for the excess absorption. The first is local excess absorption in the Galaxy. As 4C 74.26 lies at relatively low latitudes ($b = 19\overset{\circ}{.}5$), it is conceivable that the extra absorption is associated with a Galactic molecular cloud. Alternatively, the absorber could be intrinsic to the source. In PKS 2349–01 and 3C 323.1, the absorber is most likely intrinsic to the source because of their high Galactic latitudes. This is in agreement with earlier findings (Sambruna et al. 1999) that excess neutral absorption is common in radio-loud AGN and the absorbing column does not appear to be correlated with the X-ray luminosity of the source (these three objects fall in the general area occupied by radio-loud AGNs in the N_{H} *vs* L_{X} plot shown in Figure 6 of Sambruna et al. 1999).

We have also detected an Fe Kα emission line in two (possibly three) sources of our sample. In order to compare the strengths of these lines with what is found in other radio-loud and radio-quiet AGNs we plotted the rest EWs against the 2–10 keV luminosity in Figure 6. This is an update of the figure presented in Sambruna et al. (1999) and Eracleous et al. (2000). The data points represent radio-loud AGNs (Sambruna et al. 1999; Eracleous et al. 2000; Eracleous 2002, and this paper). The shaded area represents the "X-ray Baldwin effect" for radio-quiet Seyferts and QSOs and its 90% dispersion (Nandra et al. 1997c). While at $L_{\mathrm{X}} < 5 \times 10^{44}$ erg s^{-1} radio-loud AGNs have systematically lower Fe Kα EWs than radio-quiet AGNs of comparable luminosity, the situation at higher luminosities is quite unclear because of the large uncertainties in the measured EWs. There are two possible ways of viewing Figure 6: either (a) radio-loud AGNs follow their own "X-ray Baldwin effect," which is systematically offset from that of radio-quiet AGNs, or (b) radio-loud AGNs do not show a Baldwin effect at all. Unfortunately, the large uncertainties in the measured EWs, especially at high luminosities, do not allow us to distinguish between these two possibilities. Better measurements of the Fe Kα EWs of luminous radio-loud AGNs ($L_{\mathrm{X}} > 10^{45}$ erg s^{-1}) are sorely needed.

The X-ray Baldwin effect for radio-quiet AGN was interpreted by Nandra et al. (1997c) as the result of a progressive ionization of the inner accretion disk as the X-ray luminosity increases. We speculate that the lack of a similar trend for radio-loud AGN indicates that the ionization structure of the disk of radio-loud AGNs does not change significantly as the X-ray luminosity increases. This could

happen, for example, in a scenario where the dense, optically thick matter in the disk is photoionized by external illumination with a hard spectrum of low ionization parameter. If the ionization parameter in the Fe Kα emitting region is extremely low, changes in the ionizing luminosity even by an order of magnitude are accompanied by a proportional increase in the line luminosity. This would be the case if the central accretion disk is an ADAF (or similar structure) which has a low radiative efficiency and produces an X-ray luminosity that is disproportionately low compared to the accretion rate and a relatively hard spectrum. Ionization of the geometrically thin disk exterior to the ADAF by hard X-rays from the ADAF itself would thus produce the desired effect.

The above picture is supported by a number of other observational results, namely the systematically lower Fe Kα EWs and FWHMs and weaker Compton "reflection" humps of radio-loud AGNs compared to their radio-quiet counterparts (see Woźniak et al. 1998; Eracleous et al. 2000; Grandi 2002). Both of these differences can be understood in the context of a scenario in which the inner accretion disk is an ADAF rather than a geometrically thin and optically thick flow. The difference in Fe Kα EWs and Compton "reflection" strengths is then a geometrical effect resulting from the small solid angle subtended by the outer disk to the primary X-ray source (Chen & Halpern 1989; Zdziarski, Lubiński, & Smith 1999). The difference in Fe Kα FWHM follows simply from Kepler's law.

To make further progress on this problem, more and better hard X-ray spectra of radio-loud AGN are needed, especially at high luminosity. The ideal instrument for this job is *XMM-Newton*. These spectra will serve to test the X-ray Baldwin effect for this class of objects. An independent test of the above hypothesis will be afforded by the profiles of the Fe Kα lines, which would be expected to be significantly different in width and asymmetry from those of Seyfert galaxies.

We thank the anonymous referee for very helpful comments. CAH was funded by a fellowship from the Schreyer Honors College of the Pennsylvania State University and by NASA grants NAG5-9133 and NAG5-27017. This work was also partially supported by NASA grants NAG5-8369 and NAG5-10817. We have made use of the NASA/IPAC Extragalactic Database (NED) which is operated by the Jet Propulsion Laboratory, California Institute of Technology, under contract with the National Aeronautics and Space Administration.

REFERENCES

Antonucci, R. R. J. 1985, ApJS, 59, 499
Arnaud, K. 1996, in ASP Conf. Ser. 101, Astronomical Data Analysis Software and Systems V, eds. G. Jacoby & J. Barnes (San Francisco: ASP), 17
Bahcall, J. N. et al. 1995, ApJ, 452, L91
Blackburn, J. K., Greene, E. A., & Pence, B. 1994, User's Guide to `FTOOLS` (Greenbelt: GSFC)
Blandford, R. D. & Begelman, M. C. 1999, MNRAS, 303, L1
Blandford, R. D. & Levinson, A. 1995, ApJ, 441, 79
Blandford, R. D. & Payne, D. G. 1982, MNRAS, 199, 883
Blandford, R. D. & Znajek, R. L. 1977, MNRAS, 179, 433
Brinkmann, W., Otani, C., Wagner, S. J., & Siebert, J. 1998, å, 330, 67
Chen, K. & Halpern, J. P. 1989, ApJ, 344, 155
Done, C., Mulchaey, J. S., Mushotzky, R. F. & Arnaud, K. A. 1992, ApJ 395, 275
Eracleous, M. & Halpern, J. P. 1998, ApJ, 505, 577
Eracleous, M. 2002, in "Mass Outflows in Active Galactic Nuclei: New Perspectives", eds. D. M. Crenshaw, S. B. Kramer, & I. M. George (San Francisco: ASP), in press
Eracleous, M., Halpern, J. P., & Livio, M. 1996, ApJ, 459, 89
Eracleous, M., Sambruna, R. M., & Mushotzky, R. F. 2000, ApJ, 537, 654
Fabian, A. C. & Rees, M. J. 1995, MNRAS, 277, L55
Favata F. 1997, A Guide to *SAX*/LECS Data Analysis
Fiore F., Guainazzi, M., Grandi P., 1999, *Cookbook for BeppoSAX NFI Spectral Analysis v.1.2*
George, I.M & Fabian, A.C., 1991, MNRAS, 249,352
George, I. M., Turner, T. J., Netzer, H., Nandra, K., Mushotzky, R. F., & Yaqoob, T. 1998, ApJS, 114, 73
Grandi, P. 2002, in "X-ray Astronomy 1999: Stellar Endpoints, AGN and the Diffuse Background", in press (astro-ph/0005577)
Guilbert,P.W. & Rees, M.J. 1988, MNRAS, 233, 475
Ingham, J. 1994, The `XSELECT` User's Guide (Greenbelt: GSFC)
Kellerman, K. I., Sramek, R. A., Schmidt, M., Green, R. F., & Shaffer, D. B. 1994, AJ, 108, 1163
Lara, L., Cotton, W. D., Feretti, L., Giovannini, G., Marcaide, J. M., Márquez, I., & Venturi, I. 2002, A&A, 370, 409
Leighly, K. M. 1999, ApJS, 125, 297
Lightman, A.P. & White, T.R. 1988, ApJ, 335, 57
Livio, M. 1997 in "Accretion Phenomena and Related Outflows," IAU Colloquium 163, ASP Conf. Ser. 121, eds D. T. Wickramasinghe, G. V. Bicknell, and L. Ferrario (San Francisco: ASP), 845
Magdziarz, P., & Zdziarski, A.A. 1995, MNRAS, 233, 837
Meier, D. L. 1999, ApJ, 522, 753
Morrison, R. & McCammon, D. 1983, ApJ, 270, 119
Nandra, K., George, I. M., Mushotzky, R. F., Turner, T. J., & Yaqoob, T. 1997a, ApJ, 476, 70
Nandra, K., George, I. M., Mushotzky, R. F., Turner, T. J., & Yaqoob, T. 1997b, ApJ, 477, 602
Nandra, K., George, I. M., Mushotzky, R. F., Turner, T. J., & Yaqoob, T. 1997c, ApJ, 488, L91
Nandra, K. & Pounds, K. A. 1994, MNRAS, 268, 405
Narayan, R. & Yi, I. 1994, ApJ, 443, L41
Narayan, R. & Yi, I. 1995, ApJ, 444, 231
Palma, C., Bauer, F. E., Cotton, W. D., Bridle, A. H., Majewski, S. R., & Sarazin, C. L. 2000, ApJ, 119, 2068
Pearson, T. J., Blundell, K. M., Riley, J. M., & Warner, P. J. 1992 MNRAS, 259, 13P
Rees, M. J., Begelman, M. C., Blandford, R. D., & Phinney, E. S. 1982, Nature, 295, 17
Reynolds C. S., 1997, MNRAS, 286, 513
Riley, J. M. & Warner, P. J. 1990, MNRAS, 246, 1
Riley, J. M., Warner, P. J., Rawlings, S. Saunders, R., & Pooley, G. G. 1988
Sambruna, R. M., Eracleous, M., & Mushotzky, R. F. 1999, ApJ, 526, 60
Turner, T. J., George, I. M., Nandra, K., & Turcan, D. 1999, ApJ, 524, 667
Yaqoob, T., et al. 2000, *ASCA* GOF Calibration Memo ASCA-CAL-00-06-01, v1.0, `http://heasarc.gsfc.nasa.gov/docs/asca/calibration/nhparam.html`
Wilson, A. S. & Colbert, E. J. M. 1995, ApJ, 438, 62
Woźniak, P. R., Zdziarski, A. A., Smith, D., Madejski, G. H., & Johnson, W. N. 1998, MNRAS, 299, 449.
Zdziarski, A. A. & Grandi, P. 2001, ApJ, 551, 186
Zdziarski, A. A., Johnson, N. W., Done, C., Smith, D., & McNaron-Brown, K. 1995, ApJ, 438, L63
Zdziarski, A. A., Lubiński, P., & Smith, D. A. 1999, MNRAS, 303, L11

TABLE 1
TARGET PROPERTIES AND OBSERVATION DETAILS

z	Galactic $N_{\rm H}$ ($\rm cm^{-2}$)	Instrument	Energy Band (keV)	Expos. Time (ks)	Count Rate ($\rm s^{-1}$)	Start Date and Time (UT)
			PKS 2349–01			
0.174	3.26×10^{20}	*ASCA* GIS2	0.95–10	71.47	0.149±0.002	1999/12/24
		GIS3	0.95–10	71.45	0.188±0.002	05:24
		SIS0	0.85–8	62.36	0.272±0.002	
		SIS1	1.35–8	62.30	0.220±0.002	
			3C 323.1			
0.264	2.32×10^{20}	*ASCA* GIS2	0.95–10	41.84	0.125±0.002	2000/02/08
		GIS3	0.95–10	41.86	0.152±0.002	00:35
		SIS0	0.85–8	37.37	0.222±0.003	
		SIS1	1.35–8	37.46	0.184±0.003	
			4C 74.16			
0.104	1.19×10^{21}	*SAX* LECS	0.40–4	44.50	0.161±0.002	1999/05/17
		MECS	1.65–10.5	100.28	0.308±0.002	02:53
		PDS	15–125	100.00	0.52±0.04	

TABLE 2
BEST-FITTING CONTINUUM MODELS AND PARAMETERS

Best-Fitting Models and Parameters[a]	Observed Flux[b] (10^{-12} erg s^{-1} cm^{-2})		Luminosity[b] (10^{45} erg s^{-1})		χ^2_r (d.o.f.)
	0.5–2 keV	2–10 keV	0.5–2 keV	2–10 keV	
PKS 2349–01					
Absorbed power law $N_H^{exc.} = (9 \pm 5) \times 10^{20}$cm^{-2} $\Gamma = 1.87 \pm 0.04$	3.3	6.8	0.47	0.97	1.05 (250)
3C 323.1					
Absorbed power law $N_H^{exc.} = (6 \pm 5) \times 10^{20}$cm^{-2} $\Gamma = 1.86\ ^{+0.02}_{-0.04}$	3.2	5.5	1.09	1.87	1.12 (278)
4C 74.26					
Absorbed power law plus Compton reflection $N_H^{exc.} = (3.0 \pm 0.3) \times 10^{21}$cm^{-2} $\Gamma = 1.85 \pm ^{+0.05}_{-0.04}$ Reprocessor Solid Angle, $\Omega/2\pi = 1.2^{+0.6}_{-0.5}$ Reprocessor Inclination Angle, $i = 43°$[c] Power-Law Folding Energy > 140 keV	15.1	14.1	0.74	0.69	1.07 (105)

[a] All error bars correspond to 90% confidence limits. The quoted absorbing column is in excess of the Galactic column and is assumed to be due to neutral gas at the redshift of the source.

[b] The observed flux is not corrected for absorption, while the luminosity is corrected for absorption. All bandapasses refer to the observer's frame.

[c] The inclination angle of the disk was inferred from the radio morphology and held fixed for the purpose of estimating the error bars given here. Its effect on the measured value of $\Omega/2\pi$ is explored separately in Figure 4.

TABLE 3
GAUSSIAN MODEL PARAMETERS FOR FE Kα EMISSION LINES[a]

Telescope	Rest Energy (keV)	FWHM (10^4 km s^{-1})	Rest EW (eV)	Continuum Model
		PKS 2349–01		
ASCA	$6.2^{+0.3}_{-0.2}$	6^{+6}_{-3}	230 ± 120	simple power law
ASCA	$6.2^{+0.3}_{-0.2}$	4 (< 15)	90^{+90}_{-70}	power law + "reflection" ($\Omega = 2\pi$)
ASCA	$6.2^{+0.3}_{-0.2}$	unconstr.	< 200 [b]	power law + "reflection" ($\Omega = 4\pi$)
		3C 323.1		
ASCA	6.4 (fixed)	< 13 [c]	90^{+90}_{-80} [c]	simple power law
		4C 74.26		
BeppoSAX	$6.7^{+0.2}_{-0.4}$	5 (< 15)	170^{+180}_{-100}	power law + "reflection" (Table 1)
ASCA [d]	6.4 (fixed)	60^{+120}_{-30}	250^{+400}_{-120}	power law + "reflection" ($\Omega = 2\pi$)
ASCA [d,e]	6.7 (fixed)	80^{+100}_{-80}	290^{+410}_{-140}	power law + "reflection" ($\Omega = 2\pi$)

[a] All error bars and upper limits correspond to the 90% confidence intervals, unless otherwise noted.

[b] The upper limit to the rest EW in the latter case corresponds to a FWHM of 5×10^4 km s^{-1}.

[c] In the case of 3C 323.1 a line is detected only at 90% confidence and only when we fix the rest energy at 6.4 keV. The FWHM is unconstrained at 90% confidence; the quoted limit corresponds to the 68% confidence interval. The quoted value of the EW is based on the assumption that FWHM $= 5 \times 10^4$ km s^{-1}.

[d] From the re-analysis of the data already published by Brinkmann et al. (1998) and Sambruna et al. (1999). See §3.3 for details.

[e] The line properties are unconstrained at 90% confidence. The error bars given here correspond to 68% confidence.

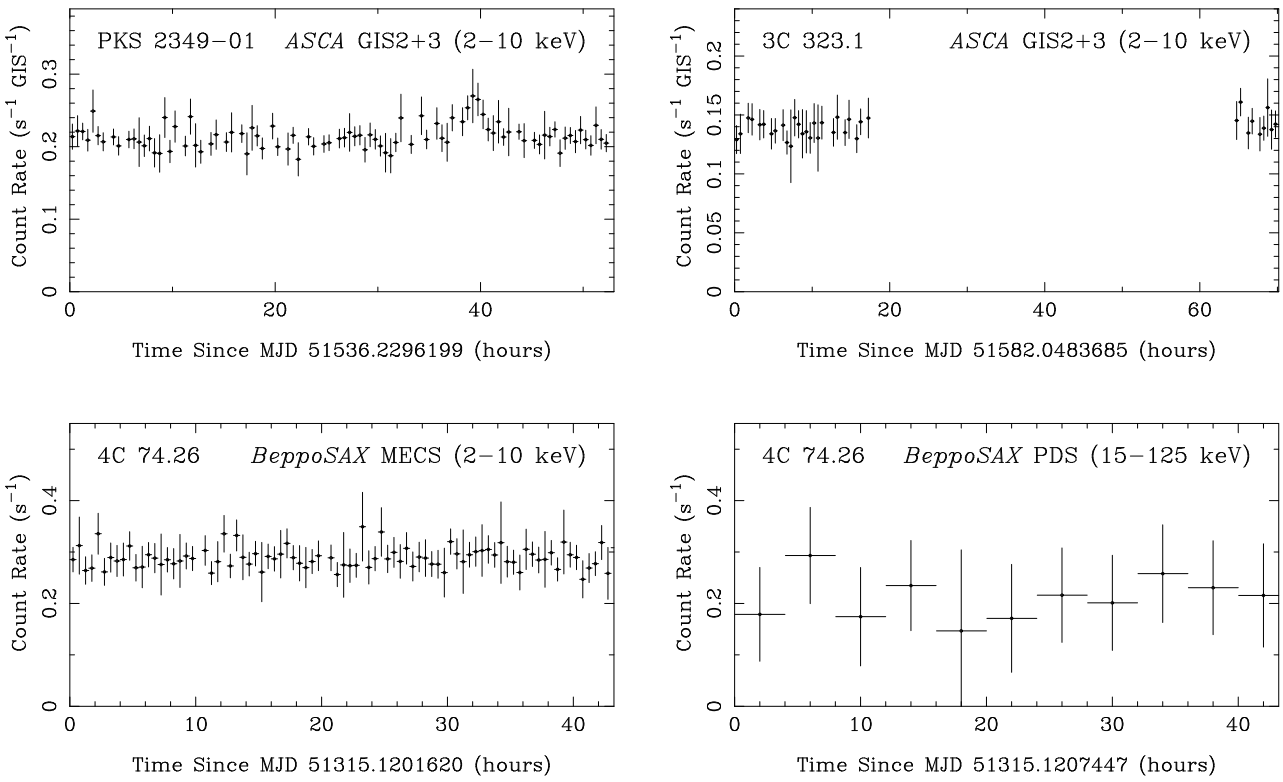

FIG. 1.— Light curves of the three quasars. The light curves of PKS 2349–01 and 3C 323.1 show the average 2–10 keV count rate from the two GIS instruments. In the case of 4C 74.26 we show a separate light curve from two of the *BeppoSAX* instruments: 2–10 keV (MECS) and 15–125 keV (PDS).

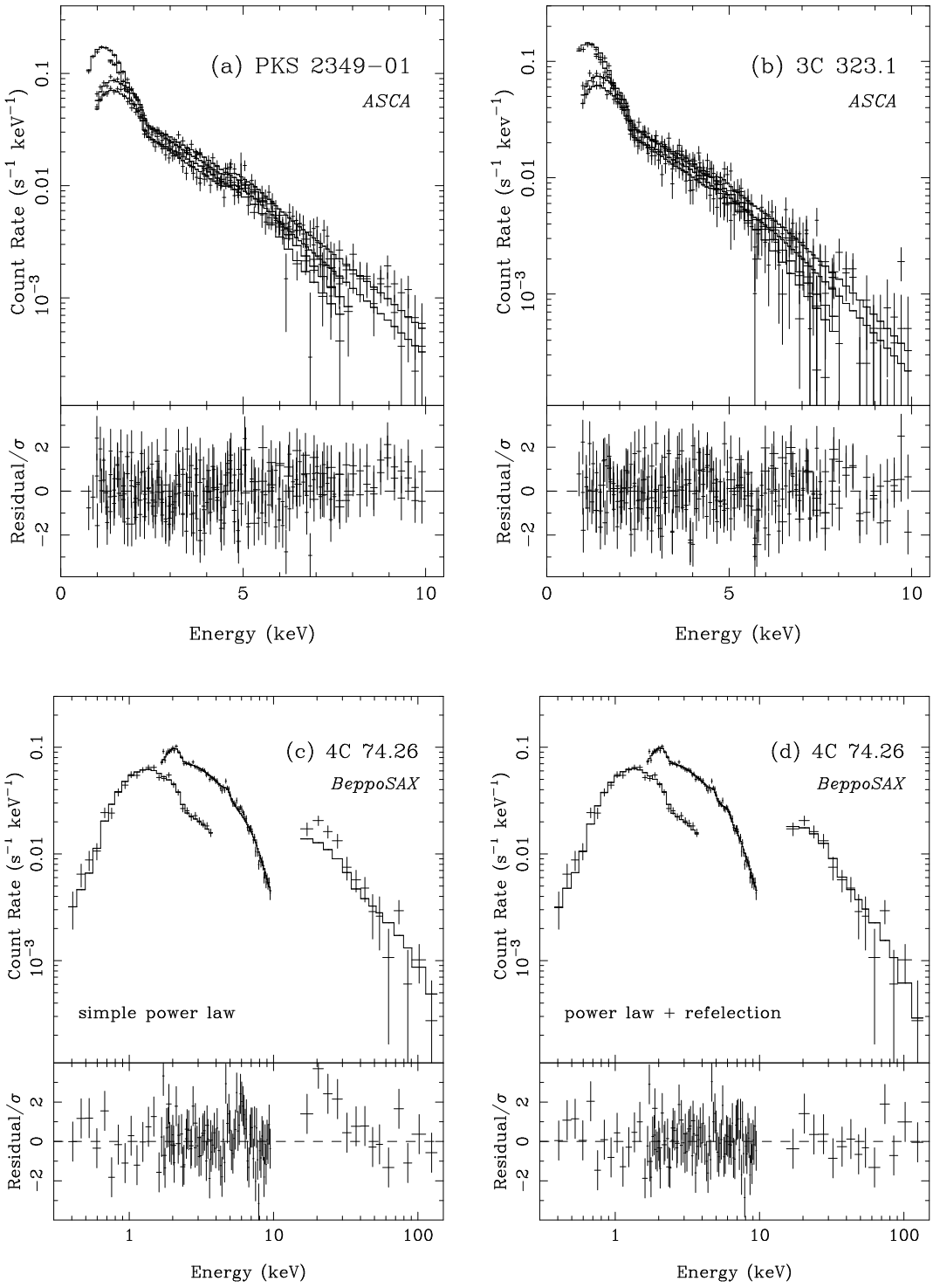

FIG. 2.— Spectra of the three quasars with models superposed. In panels (a) and (b) we show fits to the *ASCA* spectra of PKS 2349–01 and 3C 323.1 with a model consisting of an absorbed power law plus a Gaussian emission line. In panel (c) we show a simple power-law fit to the *BeppoSAX* spectrum of 4C 74.26, which leaves large residuals, especially at high energies. Panel (d) shows the *BeppoSAX* spectrum of 4C 74.26 with a model consisting of an absorbed power law plus Compton "reflection" and a Gaussian Fe Kα line which yields a considerably better fit than the simple power-law model.

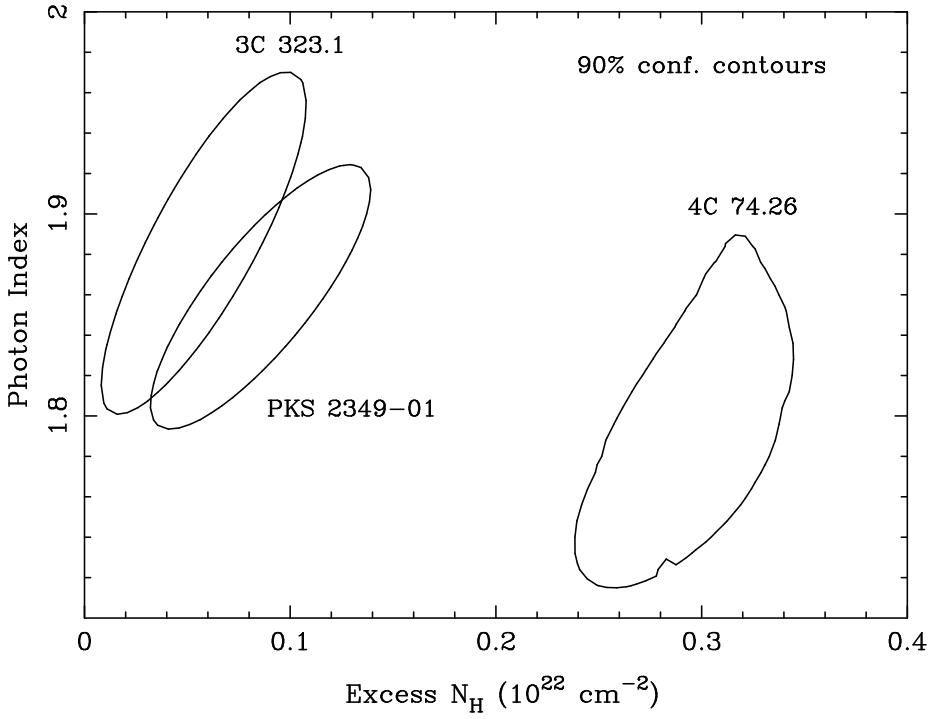

FIG. 3.— Contours showing the 90% confidence intervals in the excess absorption *vs* photon index parameter plane. The excess absorbing column is in addition to the Galactic column listed in Table 1. The contours for PKS 2349–01 and 3C 323.1 were derived by fitting the spectra from all *ASCA* instruments simultaneously, while the contours for 4C 74.26 were derived by fitting the *BeppoSAX* LECS and MECS spectra simultaneously.

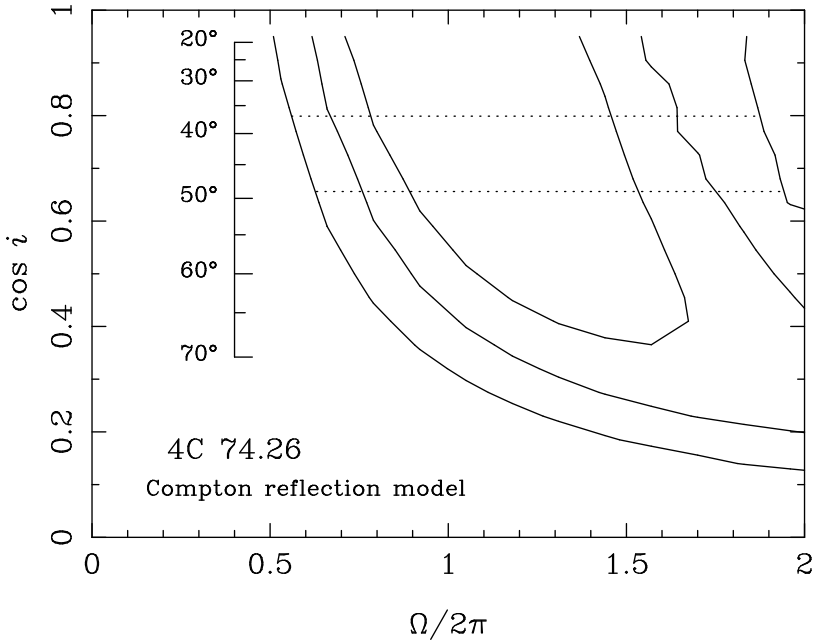

FIG. 4.— Contours showing the 68, 90, and 99% confidence intervals in the inclination angle *vs* solid angle parameter plane for the Compton "reflection" model applied to 4C 74.26. The primary power-law index and absorbing column density were allowed to vary during the fit but the upper cut-off energy of the primary spectrum was held fixed at 140 keV. The horizontal dotted lines show the range of inclination angles allowed by the radio properties (see the discussion in §3.1 of the text).

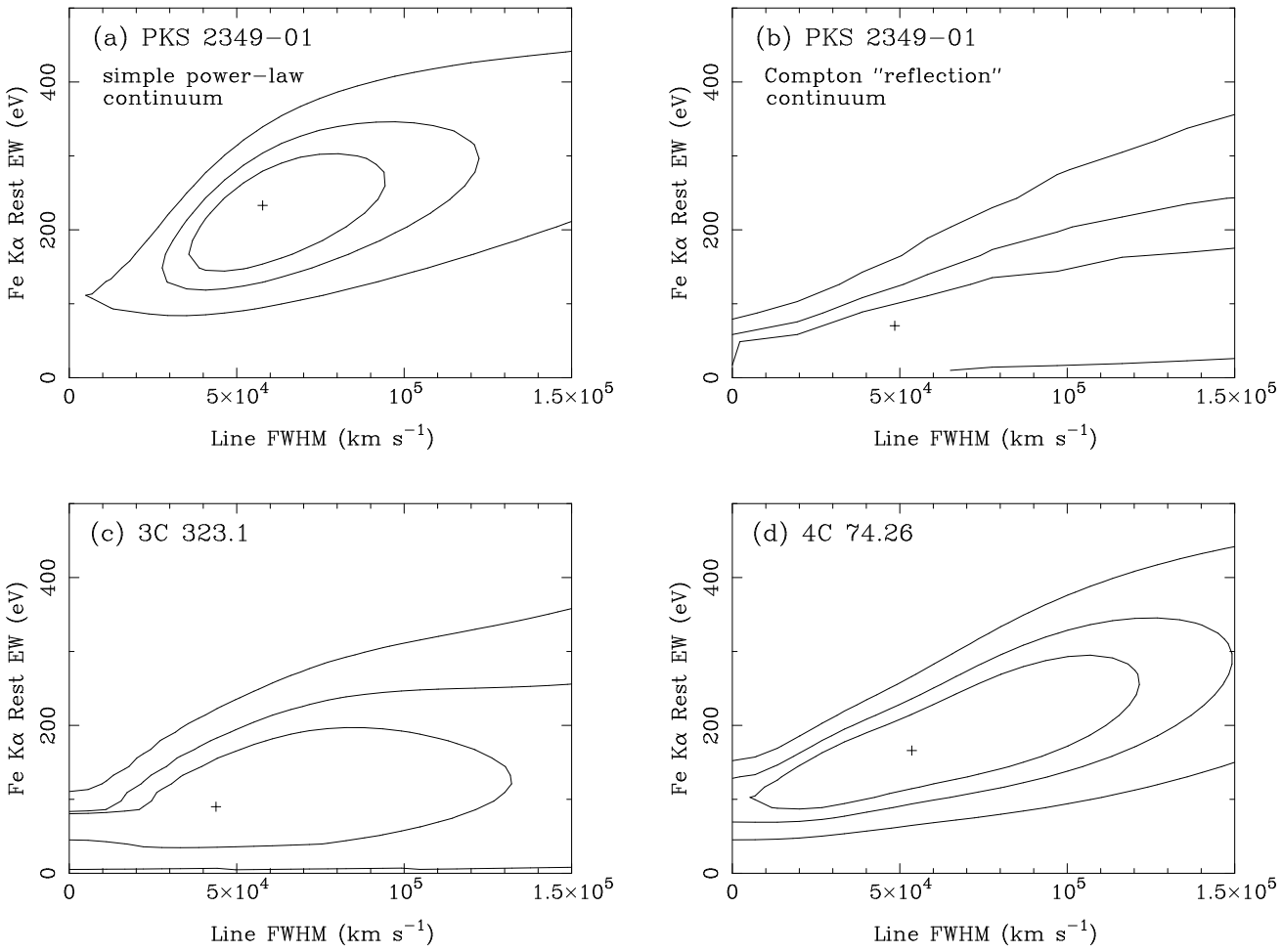

FIG. 5.— Contours showing the 68, 90, and 99% confidence intervals in the rest EW *vs* FWHM plane for the Gaussian emission-line model applied to the three quasars. The confidence intervals were obtained after fixing the parameters describing the continuum (see §3.1 of the text for details). The two panels for PKS 2349–01 refer to different continuum models: a simple power-law and a Compton "reflection" model. The panel for 3C 323.1 refers to s simple power-law model, while the panel for 4C 74.26 refers to a Compton "reflection" model. Additional details are given in the text.

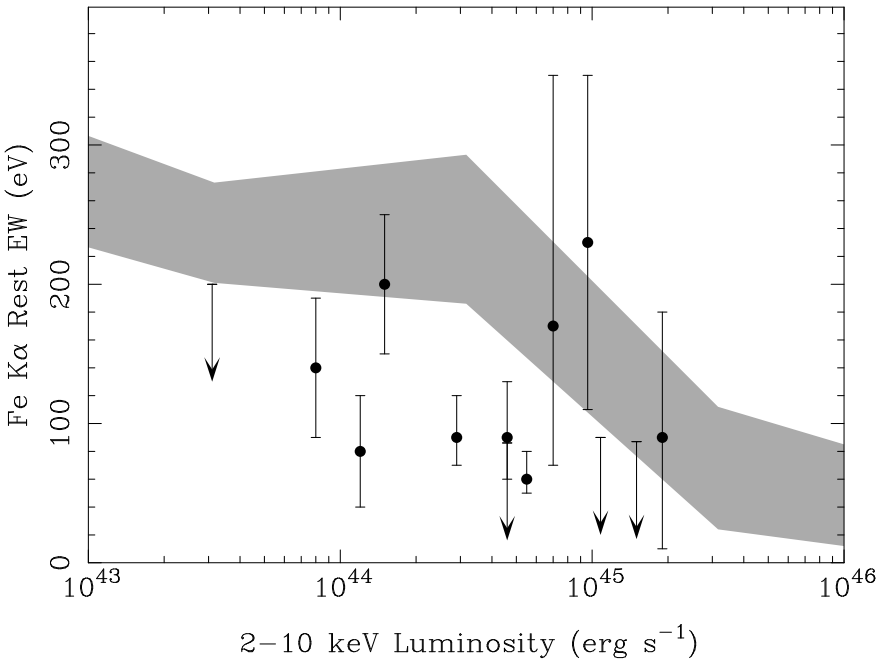

FIG. 6.— Comparison of the trends between the Fe Kα rest EW and 2–10 keV luminosity in radio-quiet and radio-loud AGNs. The grey band shows the region of this diagram occupied by the sample of Nandra et al. (1997c), which consists primarily of radio-quiet AGNs at $L_{\rm X} < 10^{45}$ erg s^{-1}. The data points represent radio-loud AGNs from this paper and earlier papers in our program, as follows: Arp 102B (upper limit at $L_{\rm X} = 3 \times 10^{43}$ erg s^{-1}; from Eracleous 2002), 3C 445 and 3C 390.3 (EW $\approx$ 140 and 200 eV; from Sambruna et al. 1999), Pictor A, 3C 120, 3C 382, 3C 111 (EW $\lesssim$ 100 eV and 10^{44} erg s^{-1} $< L_{\rm X} < 10^{45}$ erg s^{-1}; from Eracleous et al. 2000), 3C 249.1, 3C 109, 3C 254 (upper limits at 4×10^{44} erg s^{-1} $< L_{\rm X} < 2 \times 10^{45}$ erg s^{-1}; from Sambruna et al. 1999), 4C 74.26, PKS 2349–01, and 3C 323.1 (large error bars at $L_{\rm X} > 7 \times 10^{44}$ erg s^{-1}; from this paper). At $L_{\rm X} < 5 \times 10^{44}$ erg s^{-1} the radio-loud AGNs fall systematically below the trend defined by the radio-quiet AGNs, while at higher luminsoities the situtation is unclear.